© 2018 IJSRSET | Volume 4 | Issue 9 | Print ISSN: 2395-1990 | Online ISSN : 2394-4099
Themed Section : Engineering and Technology

Tissue Compensation Approach with Perspex Slab for External Beam Radiotherapy

Samuel Nii Adu Tagoe*[1], Samuel Yeboah Mensah[1], John Justice Fletcher[2], Evans Sasu*[3]

[1]Department of Physics, School of Physical Sciences, College of Agriculture and Natural Sciences, University of Cape Coast, Cape Coast, Ghana

[2]Department of Applied Physics, University for Development Studies, Navrongo Campus, Navrongo, Ghana

[3]National Centre for Radiotherapy Oncology and Nuclear Medicine, Korle Bu Teaching Hospital, Accra, Ghana

ABSTRACT

Skin sparing is retained by representing bolus for tissue deficit compensation with a compensator which is placed at certain distance from the skin. Owing to the position of the compensator, the shape of the compensator needs to be adjusted to account for beam divergence and reduction in scattered radiation contribution to dose at any point within the patient, such that dose distribution within the patient would be the same as that obtained with the bolus. Procedures for determining the shape and constructing Perspex (Polymethylmethaneacrylate) missing tissue compensators had been outlined for a telecobalt machine based on outputs of a forward planning treatment planning system, used to simulate irradiation geometries with boluses. The proposed approach considered the influences of treatment parameters: field size, treatment depth and bolus thickness to be applied in the determination of the required compensator material thickness along a particular ray-line. A semi-empirical algorithm based on beam data measured in full scatter water phantom with and without the compensator material, was proposed for the conversion of a bolus thickness to compensator material thickness such the dose distribution within a patient remain the same. Outputs of the proposed approach compared favourably well with those of the treatment planning system with discrepancies less than or equal to ± 3% (mean of 1.99 ± 0.64 %). The use of the proposed approach for clinical application is recommended.

Keywords: Perspex, compensating filter, bolus, telecobalt machine, missing tissue compensation

I. INTRODUCTION

The most reliable and verifiable quantity that tries to link treatment parameters to observed treatment outcomes for specific treatment technique in radiotherapy is the dose distribution within the irradiated region [1]. It is therefore imperative to device the optimal irradiation techniques which will maximize radiation dose to the intended target volume being treated, whilst concurrently minimizing doses to neighbouring tissues in close proximity to the target volume during external beam radiotherapy (EBRT). Administering suboptimal treatment or over-irradiating normal of tissues is likely to result in an unfavourable treatment outcome for the patient, at greater expense for the patient and the society as a whole [2]. Also during EBRT the spatial distribution of radiation dose within a patient is influenced by a lot of factors: such as patient surface topography at the point of beam entrance, and tissue inhomogeneities within the irradiated region of the patient [3]. Irregularities such as tissue deficit on the

patient at the point of beam entrance causes an uneven dose distribution over the tumour volume (intended target volume) and can be compensated for with a bolus. Bolus which are mostly made from tissue equivalent materials are placed on the skin of the patient during treatment delivery. An unfortunate consequence of using a bolus is the loss of skin sparing associated with megavoltage beams. Howbeit, moving the bolus from the patient surface toward the teletherapy machine radiation source (specifically the block tray position) retains the compensation of the bolus and also re-establishes the compromised skin sparing. Since the bolus is no longer in contact with the patient, it can be composed of any non-tissue equivalent material, and it is referred to as a compensating filter (or compensator) [4]. When compensating filters are used they are usually placed at distances of about 15 - 20 cm from the patient surface [4], but there are instances where they have been placed very close to the patient to increase the dose to the skin to some extent, especially in total body irradiation [5]. The dose to the skin attributed to the compensating filter increases as the separation between the compensating filter and the patient surface decreases, and the compensating filter used in this sense is referred to as a beam spoiler [4, 5]. There is reduction in scattered radiation contribution to radiation dose at any point within the patient when a compensating filter is used to represent or mimic the bolus. The reduction in the scattered radiation contribution is also influenced by certain treatment parameters, such as: field size, treatment depth, off-axis distance, bolus/compensating filter thickness, beam energy and the separation between the patient and the compensating filter. The distance from the compensating filter to the surface of the patient had been found to be the most crucial among the treatment parameters, and had been taken care of by maintaining distances within the range of 15 - 20 cm between the filter and the patient surface [4]. To achieve the same dosimetric effects as the bolus in terms of the dose distribution within the patient, the thickness of the compensating filter in the direction of propagation of the beam needs to be adjusted to account for the reduced scattered radiation contribution to dose at any point within the patient. Owing to the complexities involve in trying to account for the treatment parameters enumerated, the treatment parameters are mostly ignored when designing and constructing compensating filters for missing tissue compensation [4]. Also, due to the position of the compensating filter, the shape of the compensating filter needs to be tapered in length and width to account for beam divergence. Generally, the shape of the compensating filter is smaller than the representing bolus. A compensating filter can also be used to account for the effects of tissue inhomogeneities [3, 4], but this not part of the scope of this publication.

This paper seeks to find ways of incorporating the effects of the aforementioned treatment parameters with the exception of the off-axis distance into the design and construction of a Perspex (PMMA) compensating filter for missing tissue compensation for beams from a telecobalt machine.

A. Underpinning Principle:

In designing compensating filter, the objective is to ensure that the thickness of the compensating filter material absorbs the equivalent amount of radiation as the thickness of tissue missing from the patient as depicted in figure 1. If the thickness of the compensating filter along a particular ray line in figure 1 is found to be, t and that of the missing tissue (or tissue deficit) is T , the thickness ratio or density ratio, τ is given by [4];

$$\frac{t}{T}\rho_c = \tau \qquad (1),$$

where ρ_c is the density of the compensating filter material.

The thickness (or thickness density) ratio is found to depend on a lot of factors, such as the compensating filter to surface distance, thickness of missing tissue

(or relative compensating filter thickness required), field size, treatment depth, and beam energy [4].

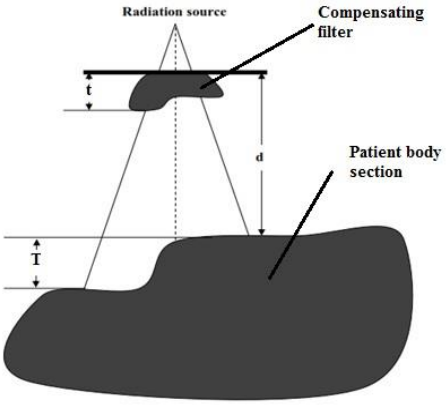

Figure 1. Schematic representation of a compensating filter designed for an irregular surface .

The thickness of compensating filter, t at a given point within a radiation field is calculated from equation (1), which is rearranged to give [4];

$$t = T\left(\tau/\rho_c\right) \qquad (2),$$

where T is the tissue deficit at the point considered and ρ_c is the density of the compensating filter material. T can be simulated with a bolus thickness regarded the bolus is composed of a tissue equivalent material (with density similar to that of water).

Owing to the dependences of, τ , a direct determination of thickness $\left(\tau/\rho_c\right)$ is to measure dose with the compensating filter mounted on a tray within the beam for appropriate depth and field size in a tissue equivalent phantom and the same measurement repeated without the compensating filter, such that the thickness of the phantom is adjusted to get the same dose as before. The ratio of compensating filter thickness to that of the adjusted thickness of the phantom gives $\left(\tau/\rho_c\right)$ [4].

II. METHODS AND MATERIAL

To ensure reproducibility of the experimental outcome, the density and mass attenuation coefficient of the Perspex used were empirically verified. For the mass attenuation coefficient the measurements were done in air for field sizes ranging from 3 cm x 3 cm to 30 cm x 30 cm. The mass attenuation coefficient for each field size was determined as the ratio of measured linear attenuation coefficient for that particular field size to the density of Perspex. The density of Perspex was determined by finding the weights of eight different samples of Perspex plates used for the study with a digital chemical balance (Mettler Toledo™ ME-TE Precision Balance; Fisher scientific, USA) and dividing the respective weights with their corresponding volumes of the Perspex plates. The volume of a plate was determined from its physical dimensions measured with a electronic digital caliper (Model # 50003; Chicago Brand Industries, USA). The mean of the densities determined was taken as the density of the Perspex used in this study.

A. Commissioning:

All beam data were measured on the beam central axis with 0.125 cc cylindrical ionization chamber (TW31002-1505; PTW-Freiburg, Germany) in a full scatter motorized water phantom, Blue Phantom^2 (IBA Dosimetry GmbH, Germany). The ionization chamber was connected to a UNIDOS electrometer (10002-20204; PTW-Freiburg, Germany), which was set to measure the output of the teletherapy machine in terms of charges at 60 seconds interval with a chamber bias voltage of + 300 V. The teletherapy machine which was used in this study and whose beam data acquired was an Equinox 100 cobalt 60 telecobalt machine (Best Theratronics, Canada). In all the measurements, it was ensured that there was at least 10.0 cm of water below the detector to provide the needed backscattered radiation. The isocentric irradiation technique was also maintained in all the measurements, and this was achieved by keeping the position of the detector constant and pumping water into the phantom to obtain the desired depth of measurement. Schematic diagram of the experimental set up is depicted in figure 2. To ensure reproducibility of the experimental outcome, the

density and mass attenuation coefficient of the Perspex used were empirically verified.

B. Thickness ratio determination:

The following measurement were done to obtain the thickness ratio for the compensating filter. Perspex plates (dimensions of 20 cm x 20 cm) with thicknesses ranging from 0 to 7.2 cm (increments of 0.8 cm) were successively mounted on a block tray and placed in the path of beams from the telecobalt machine employing isocentric irradiation technique. Each beam had a field size of 10 cm x 10 cm. The block tray was held at the accessories holder on the collimator system of the telecobalt machine. For each thickness of Perspex plate mounted the block tray, transmitted output of the telecobalt machine was measured with the ionization chamber placed at a depth of 5.0 cm within the phantom and the electrometer reading corrected for temperature and pressure influences. The above measurements were repeated without the Perspex plates, but only the block tray on which the Perspex plates were mounted. With the detector at the same depth and maintaining the isocentric irradiation technique, the height of water within the phantom was adjusted from 0 to 20 cm (increments of 2 cm). For each adjusted height of water above the detector, the electrometer reading was obtained and once again corrected for influencing factors (temperature and pressure). From these measurements, the adjusted height of water above the detector that would give the same corrected electrometer reading as that of a measurement done with a particular thickness of Perspex plate in the path of the beam was determined for each thickness of the Perspex plate used. Correlation between adjusted height of water above the detector and the corresponding thickness of Perspex that would give the same beam output was determined. The ratio of thickness of Perspex to the corresponding adjusted height of water above the detector that would give the same beam output was determined for various adjusted heights of water above the detector. A graph of thickness ratio as a function of adjusted height of water above the detector was plotted and the correlation equation as well as the regression, R^2 of the line of best fit obtained.

C. Accounting for field size variations:

To study the influence of field size (or collimator settings) on the thickness ratio, the above experimental procedures were repeated with a constant thickness of the Perspex plate mounted on the block tray and placed into the path of the beam, but the field size was varied from 3 cm x 3 cm to 35 cm x 35 cm. A constant Perspex plate thickness of 3.65 cm was used. For each field size setting the electrometer reading obtained was corrected for influencing factors (temperature and pressure). For the measurements without the Perspex plate in the path of the beam, corrected electrometer readings (beam outputs) obtained with the various adjusted heights of water above the detector were repeated for the various square field sizes. From the above measurements, the adjusted height of water above the detector for a particular field size that would give the same corrected electrometer reading as that of a measurement with the Perspex plate in the path of the beam using the same field size, was determined. For each field size, the ratio of thickness of the applied Perspex plate thickness placed in the path of the beam during the measurements to the corresponding adjusted height of water above the detector determined from measurements without the compensating filter, but the height of water above the detector adjusted to obtain the same beam output for both measurement scenarios, was calculated for the various field sizes used. The ratios obtained were normalized to that of the reference field size of: 10 cm x 10 cm. The normalized ratios were referred to as field size correction factors. Graph of field size correction factor was plotted against one side of a square field size (equivalent square field size), and correlation equation as well as regression, R^2 of the line of best fit determined.

D. Accounting for treatment depth variations:

To study the influence of treatment depth on the thickness ratio, the measurements with the varying field sizes were repeated but the field size was kept constant at 10 cm x 10 cm and the depth of measurement varied from 0.5 to 17.0 cm. For each depth of measurement with the constant thickness of Perspex plate in the path of the beam, the output of the telecobalt machine was obtained and corrected for influencing factors (temperature and pressure). For the measurements without the Perspex plate in the path of the beam, with the fixed field size, electrometer readings (telecobalt machine outputs) were obtained for measuring depths ranging from: 0.5 to 32.0 cm. The measured beam outputs (electrometer readings) for the various measuring depths were corrected for variations in air density. From these measurements, for each depth of measurement with the Perspex plate in the path of the beam, a corresponding depth of measurement without the plate in the path of the beam that would give the same corrected electrometer reading as that with the Perspex plate in the path of the beam was determined. The depth of measurement with the Perspex plate in the path of the beam was subtracted from the determined corresponding depth of measurement without the plate in the path of the beam to determine the related adjusted height of water above the detector. For each depth of measurement, the ratio of thickness of the applied Perspex plate thickness placed in the path of the beam during the measurements to the corresponding adjusted height of water above the detector determined from measurements without the compensating filter, but the height of water above the detector adjusted to obtain the same beam output for both measurement scenarios, was calculated for the various depth of measurements used. The ratios obtained were normalized to that of the depth of measurement of 5.0 cm with the Perspex plate in the path of the beam. The normalized ratios were referred to as treatment depth correction factors. A graph of treatment depth correction factor was plotted against depth of measurement with the Perspex plate in the path of the beam (treatment depth), and the correlation equation as well as the regression, R^2 of the line of best fit determined.

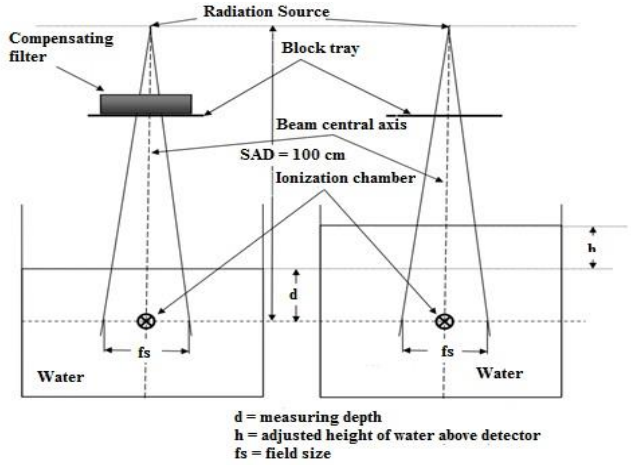

Figure 2. Schematic diagram of experimental set up.

E. Compensating filter construction:

In constructing the compensating filter, the length and width were tapered to account for beam divergence. To achieve this, a compensating filter sheet with grid lines having grid area of 1 cm x 1 cm, and two perpendicular lines running through the central part to represent the major axes of a beam, was designed to record the applied bolus thicknesses along the surface of a patient. The grid area covered an area of about 2 cm x 2 cm at the isocentre of telecobalt machine. The thickness of the compensating filter along the direction of propagation of the beam was also tapered, to account for the reduction of scattered radiation contribution to radiation dose at any point within the patient for using the compensating filter to represent the bolus of the TPS during the treatment planning process. After determining the bolus thickness, x_b within each grid and using equation (2), the thickness, x_c of a compensating filter along the grid was determined as:

$$x_c = T_{t_b} f_r f_d x_b \quad (3),$$

where f_d is the treatment depth correction factor applicable to a specified treatment depth; it was represented generally by the correlation equation determined from the plot of depth correction factor against treatment depth for the compensating filter

material under consideration, f_r is the field size correction factor applicable to a particular field size (equivalent square field) used; it was represented generally by the correlation equation determined from the plot of field size correction factor against field size for the compensating filter material under consideration, and T_{t_b} is the appropriate thickness ratio for a particular thickness of bolus applied within a grid (or along a ray line) under reference conditions (field size of 10 cm x 10 cm and treatment depth of 5 cm); this was represented by the correlation equation determined from the plot of thickness ratio against adjusted height of water above the detector.

Once the thicknesses of the compensating filter at various portions of the radiation field to be modulated had been determined and recorded within the respective grids of the compensating filter sheet, the compensating filter sheet with the recorded thicknesses was pasted at the back of transparent Perspex block tray in use for the telecobalt machine, such that a beam central axis inscribed on the surface of the block tray matched that of the compensating filter sheet. The block tray was similar to what was used during the commissioning process. Samples of Perspex plates used for the commissioning having dimensions of 1 cm x 1 cm but different thicknesses, were stacked together on the block tray to obtain the stipulated thicknesses of Perspex within the various grids. The Perspex plates or blocks were held in place with an adhesive (or bonding agent) and in this case Chloroform (or Trichloromethane) was used.

F. Simulation of implementation of compensating filter:

Treatment simulations were performed with Prowess Panther TPS, version 4.6 (Prowess Inc., USA). A phantom with dimensions of: 30 cm x 30 cm x 20 cm with radiological properties similar to an acrylic slab phantom which would be used to verify treatment plans, was created with the TPS using a slice thickness of 5 mm. After the outline of the phantom had been delineated on each slice with the auto-contouring tool, multiple plans were generated for the phantom using the plan manager tool. Each plan had a single anterior beam employing SAD treatment technique, but the field size and treatment depth (dose prescription depth) for the various plans were different. The plans were named plan 1, plan 2, plan 3, plan 4 and plan 5. For plan 1, a field size of 10 cm x 10 cm and a treatment depth of 5 cm (with dose of 1.0 Gy normalized to the isocenter) were used. In plan 2, the field size was 15 cm x 6 cm and the treatment depth was 7 cm with a prescribe dose of 1.5 Gy normalized to the isocenter. For plan 3, a field size of 25 cm x 15 cm and a treatment depth of 10 cm were used to deliver a prescribed dose of 2.0 Gy at the isocenter. For plan 4, a field size of 25 cm x 25 cm and a treatment depth of 15 cm were used to deliver a prescribed dose of 2.5 Gy at the isocenter. Finally, for plan 5, a field size of 23 cm x 4 cm and a treatment depth of 3 cm were used to deliver a prescribed dose of 2.5 Gy at the isocenter. During the treatment planning processes with the TPS, missing tissue compensation were achieved by placing bolus shaped in the form of step wedges on the surface of the phantom at the point of beam entrance. It was ensured in each case that the area covered by the bolus extended about 2 cm beyond the radiation field limits (field edges) indicated on the surface of the phantom. Prior to the creation of the bolus, the Hounsfield unit of the bolus material was set to that of water (HU= 0), which was the default for the TPS.
Axial view of the shape of the bolus per case scenario is depicted in the planning windows shown in figure 3. For each of the plans, the beam central axis was made central to the phantom, and the beam incident normal to the surface of the phantom. Dose calculation points were then placed at the isocenter along the beam major axis in the direction of the steps of the step wedge bolus. Starting from the beam isocenter, the calculation points were placed at 2 cm part from each other on either side of the beam central axis as shown in figure 3.A and 3.B respectively. The step wedges were created such that the middle of the steps were closely in line with the

calculation points placed along the beam major axis at the isocenter. Two types of step wedges were created with the bolus and the step wedges were referred to as scenarios case 1 and 2 respectively. The various plans were repeated with each type of step wedge of the bolus on the phantom. With the various prescribed doses and irradiation geometries, dose distributions within the phantom were calculated with the TPS and the corresponding treatment times recorded for the various plans. The off-axis dose profiles along the isocenter in the direction of the step wedge together with their corresponding off-axis distances from the beam central axis were also recorded. Bolus thicknesses along the surface of the phantom for the various grids were determined with aid of special inherent graduated patient registration tool of the TPS, which were converted to compensating filter thicknesses using equation (3) to facilitate the construction of the compensating filter for each plan.

The various treatment plans were replicated on the telecobalt machine with the bolus replaced by appropriate Perspex compensating filters, constructed based on the proposed approach, placed in the path of the beam, and the off-axis doses measured with calibrated Gafchromic EBT2 film samples (Lot #: 08221302; Ashland Inc., USA). The Gafchromic EBT2 film was calibrated against a 0.6 cc cylindrical ionization chamber (TW 30013; PTW Freiburg, Germany) having traceability to a secondary standard laboratory, based on the International Atomic Energy Agency (IAEA) technical report series (TRS) 398 protocol [17]. The optical densities of exposed films were read with ImageJ analyzing software (National Institutes of Health, USA) and the optical densities obtained converted to doses using the sensitometric curve of the film obtained during the calibration process. The exposed films were scanned with flatbed scanner, ScanMaker® 9800XL plus (Microtek, USA), and the images saved in Tagged Image File Format (TIFF) prior to the analysis with the ImageJ software. During the dose measurements, the films were sandwiched between the piles of the acrylic slabs forming the phantom (T2967; PTW Freiburg, Germany) at the required treatment depth and were held in place by gravity on the treatment couch of the telecobalt machine.

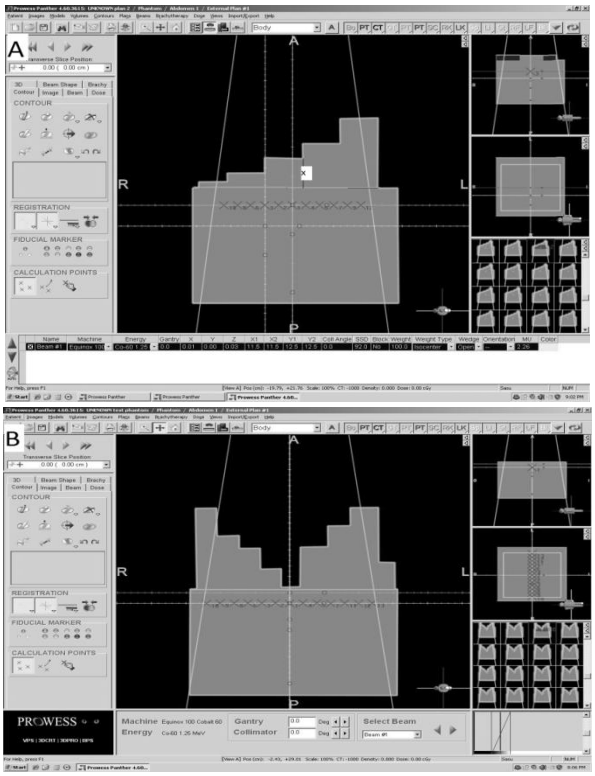

Figure 3. TPS planning window showing plans for dosimetry verification; A; bolus shape for case 1; and B; bolus shape for case 2.

III. RESULTS AND DISCUSSION

Figure 4 shows the variation of compensating filter (or Perspex plate) thickness as a function of adjusted height of water above the detector. Above the curve in figure 4 is displayed the correlation equation (coefficient) as well as the regression, R^2 of the line of best fit.

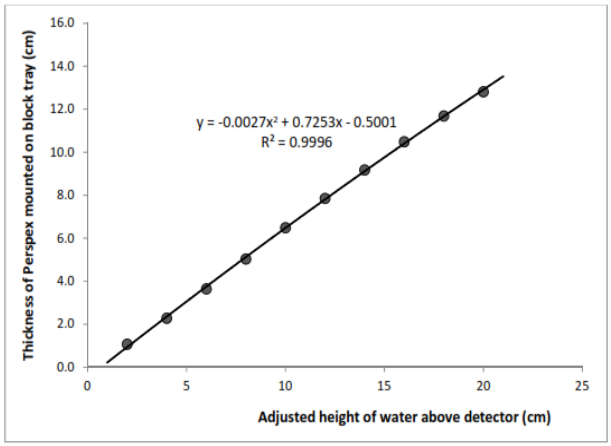

Figure 4. Variation of compensating filter thickness as a function of adjusted height of above detector.

A graph of ratio of compensating filter thickness to adjusted height of water above the detector (thickness ratio) against adjusted height of water above the detector or simulated bolus thickness is depicted in figure 5. Above the curve shown in figure 5 are correlation equation and the regression, R^2 of the line of best fit.

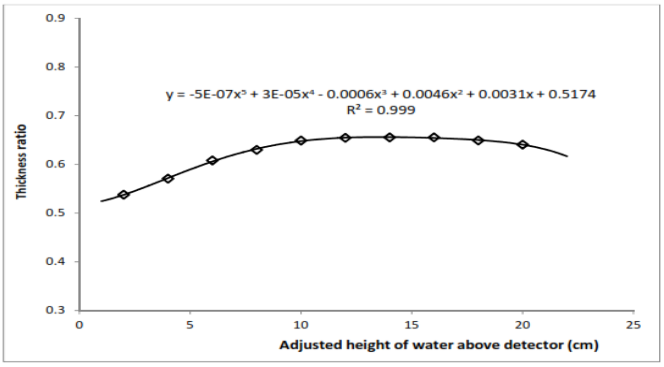

Figure 5. Graph of thickness ratio against adjusted height of water above chamber or simulated bolus thickness

In figure 6 is shown a graph of field size correction factor as a function of one side of a square field size. Above the curve depicted in figure 6 are the correlation equation and the regression, R^2 of the line of best fit.

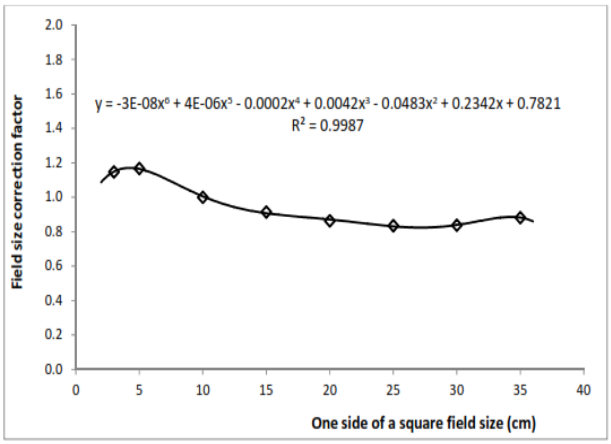

Figure 6. Graph of field size correction factor as a function of field size.

In figure 7 is depicted a graph of treatment depth correction factor against depth of measurement within the water phantom. Also above the curve in figure 7 are displayed the correlation equation and the regression, R^2 of the line of best fit.

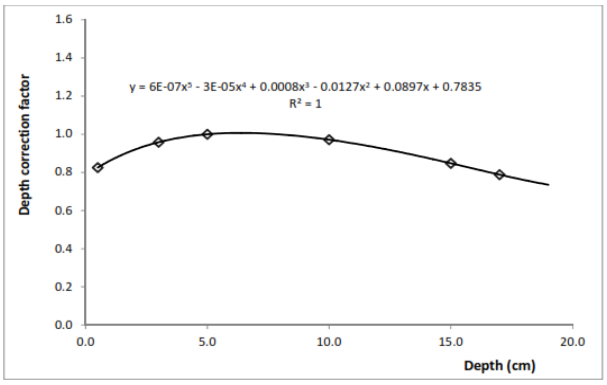

Figure 7. Graph treatment depth correction factor as a function of treatment depth

From the graphical manipulations and curve fitting analyses performed on the experimental data obtained, the various terms in equation (3), which was proposed for converting applied bolus thickness to Perspex compensating filter thickness are given as:

$$T_{t_b} = (-5 \times 10^{-7}){t_b}^5 + (3 \times 10^{-5}){t_b}^4 - (0.0006){t_b}^3 + (0.0046){t_b}^2 + (0.0031)t_b + 0.5174 \quad (4),$$

$$f_r = (-3 \times 10^{-8})r^6 + (4 \times 10^{-6})r^5 - (0.0002)r^4 + (0.0042)r^3 - (0.0483)r^2 + (0.2342)r + 0.7821 \quad (5), \text{ and}$$

$f_d = (6 \times 10^{-7})d^5 - (3 \times 10^{-5})d^4 + (0.0008)d^3 - (0.0127)d^2 + (0.0897)d + 0.7835$ (6),

where t_b , r and d are applied bolus thickness within a grid of the compensating filter sheet, equivalent square field size and treatment depth respectively.

In figure 8 below is shown a plot of the variation of measured mass attenuation coefficient in air with field size for Perspex. Above the curve depicted in figure 8 are the correlation equation and the regression, R^2 of the line of best fit.

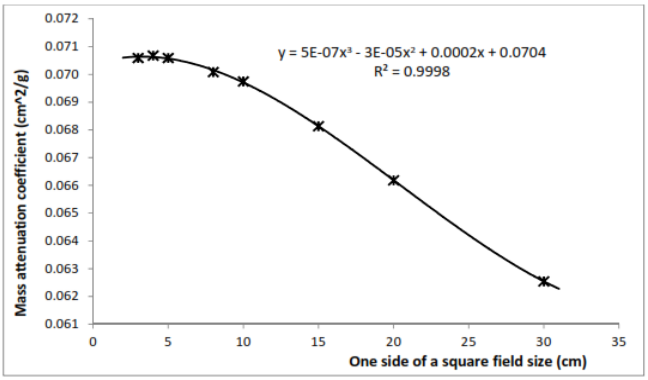

Figure 8. Variation of mass attenuation coefficient with field size.

The measured doses at the various calculation points (Calc. Pt #) with the Gafchromic films for using the compensating filter to represent the bolus of plans generated with the TPS, and the treatment plans replicated on the teletherapy machine, are presented in tables 1 for the various treatment plans (Plan #) and case scenarios. The calculated doses represent doses calculated with the TPS with bolus on the surface of the phantom at the point of entrance of beams. Also presented in table 1 are the discrepancies between the calculated and the measured doses for the various calculation points, which are expressed as percentage differences of the respective measured doses. These are enumerated for the various treatment plans and case scenarios. For case 1 the discrepancies ranged from: - 1.78 to 3.00 % (mean of ± (1.89 ± 0.76) %). And for case 2 the discrepancies ranged from: - 2.80 to 3.00 % (mean of: ± (2.08 ± 0.50) %).

The omissions in table 1 indicate places where the calculation points fall outside the steps of the step wedge bolus generated with the TPS.

Table 1. Comparison Of Doses

Plan #	Calc. Pt #	Calculated dose (cGy)		Measured doses (cGy)		%Diff. between measured and calculated doses	
		Case 1	Case 2	Case 1	Case 2	Case 1	Case 2
1							
	1	100.00	100.00	100.00	101.01	0.00	1.00
	2	98.38	85.08	99.57	87.07	1.20	2.28
	3	92.06	80.29	94.03	78.29	2.10	-2.56
	4	86.56	69.38	85.51	70.70	-1.23	1.87
	5	82.54	66.79	84.52	68.39	2.34	2.34
2							
	1	150.00	150.00	151.32	152.86	0.87	1.87
	2	148.15	125.75	152.73	128.15	3.00	1.87
	3	146.37	123.47	150.22	125.72	2.56	1.79
	4	129.54	99.70	131.46	101.38	1.46	1.66
	5	126.30	98.48	128.33	100.16	1.58	1.68
	6	159.70	94.90	164.10	96.82	2.68	1.98
	7	121.	94.8	123.	97.1	2.0	2.45

		30	0	84	8	5	
3							
	1	200.00	200.00	198.57	203.50	-0.72	1.72
	2	198.17	169.79	203.48	165.86	2.61	-2.37
	3	196.67	170.48	202.07	175.16	2.67	2.67
	4	175.36	140.83	173.66	145.16	-0.98	2.98
	5	174.27	139.99	177.97	142.91	2.08	2.04
	6	220.14	140.00	222.43	141.46	1.03	1.03
	7	173.48	138.45	177.49	141.94	2.26	2.46
	8	214.61	136.12	220.11	138.83	2.50	1.95
	9	167.95	117.51	165.01	119.52	-1.78	1.68
	10	206.83	110.05	211.22	112.73	2.08	2.38
	11	208.25	110.82	213.11	113.41	2.28	2.28
	12	130.61	107.56	132.20	105.60	1.20	-1.86
	13	123.53	58.01	126.05	59.79	2.00	2.98
4							
	1	250.00	250.00	252.53	253.96	1.00	1.56
	2	248.60	213.25	255.76	207.44	2.80	-2.80
	3	246.85	214.02	243.32	210.96	-1.45	-1.45
	4	222.63	176.95	228.34	181.60	2.50	2.56
	5	220.48	176.70	226.60	181.75	2.70	2.78
	6	277.75	175.81	286.34	178.22	3.00	1.35
	7	219.26	173.65	223.55	177.05	1.92	1.92
	8	270.00	171.55	276.07	175.41	2.20	2.20
	9	212.27	148.02	216.51	150.37	1.96	1.56
	10	259.69	138.92	265.23	136.00	2.09	-2.15
	11	263.04	139.88	260.44	142.73	-1.00	2.00
	12	167.20	135.44	168.70	138.05	0.89	1.89
	13	158.14	122.27	162.19	125.92	2.50	2.90
5							
	1	250.00	250.00	252.47	253.24	0.98	1.28
	2	247.82	227.48	253.65	232.98	2.30	2.36
	3	247.62	226.01	254.18	230.55	2.58	1.97
	4	225.60	195.12	227.63	198.82	0.89	1.86
	5	224.56	194.58	231.51	198.33	3.00	1.89
	6	266.20	194.76	263.43	190.57	-1.05	-2.20
	7	221.67	192.11	227.77	195.99	2.68	1.98
	8	261.36	192.08	269.44	195.50	3.00	1.75

	9	185.29	171.04	189.94	176.06	2.45	2.85
	10	251.41	140.66	255.47	145.01	1.59	3.00
	11	-	161.59		165.99		2.65
	12	174.62	157.61	176.38	160.29	1.00	1.67
	13	-	116.81		119.06		1.89

The Perspex used in this study had a measured density of 1.18 ± 0.01 g/cm^3, but for field sizes ranging from: 3 cm x 3 cm to 30 cm x 30 cm, the in air measured mass attenuation coefficients were found to range from 0.06254 to 0.07068 cm^2/g (mean of: 0.06857 ± 0.00289 cm^2/g). The value of the mass attenuation coefficient generally decreases with increasing field size due to increasing scattered radiation contribution to dose at the beam central axis with field size. The scattered radiation comes from the jaws of the collimator system and the radiation source encapsulation itself. As field size increase the surface area of a particular jaw exposed to the radiation increases producing more scattered radiation. The correlation between the mass attenuation coefficient and field size can be expressed with a third order polynomial equation as depicted in figure 8. The measured density and the value of the mean mass attenuation coefficient of Perspex for the various field sizes, compared favourably well with those stated in literature [8]. The aforementioned radiological properties influence radiation scattering and absorption characteristics of the compensating filter material, and will have influence on the proposed equation for converting an applied bolus to compensating filter thickness. The constants within the various polynomial equations expressing the correction factors introduced into the proposed equation will be dependent on the radiological properties. It is therefore necessary to verify and validate the density and mass attenuation coefficient of the material being considered for the construction of the compensating filter prior to the implementation of the proposed approach. It can also be inferred that the various correction factors introduced will be dependent on beam energy (quality), as radiation scattering and absorption by an absorber is dependent on beam energy. Since the correction factors are scattered radiation related, anything that will affect the scattering will influence the correction factors. Hence the correction factors will be dependent on collimator system design of a teletherapy machine. The measurements with the adjusted heights of water above the detector were used to simulate or mimic the presence of bolus in the path of beams. Since bolus are composed of tissue equivalent material it was very convenient to use water to represent the bolus. Also representing the bolus with water made it very easy to change the thickness of the bolus during the measurements. An applied bolus thickness was used to represent tissue deficit (or missing tissue) likely to be encountered on a patient surface. The correlation equations (or coefficients) of the curves depicted in figures 5, 6 and 7 were used to express and determine: the thickness ratio one needs to apply for converting bolus thickness to compensating filter thickness for any: applied bolus thickness, the appropriate field size correction factor to be incorporated for any field size and the appropriate treatment depth correction factor to be incorporated for any treatment depth, respectively. And from the respective regression values which are closely approaching or equal to unity for the lines of best fits shown in figures 5, 6 and 7, signify that their respective correlation equations can be used to predict with great accuracy the thickness ratio, field size correction factor and treatment depth correction factor from their respective correlated treatment parameters. The depth of measurement within the water phantom is synonymous to treatment depth with regards to a patient. Using the expression for a correlation equation will facilitate the determination of a required factor from any related treatment parameter,

and also help in generalizing the proposed equation. To simplify the computational process for converting a bolus thickness to compensating filter thickness, lookup tables may be generated for the required factors, but in this study Microsoft spreadsheet (Microsoft Inc., USA) was used for the various calculations. The measurements with and without the compensating filter, had shown that the introduced correction factors for the stipulated treatment parameters could be expressed as fifth order polynomial equations in terms of treatment depth and applied bolus thickness respectively, and a sixth order polynomial in terms of field size, respectively by using the graphical considerations and the curve fitting analyses of the empirical data. Owing to the high orders of the polynomial equations, one needs to be circumspective not to use treatment parameters beyond the limits of those used for the empirical determination of the correction factors and the thickness ratio, as ignoring this will constitute uncertainties in a determined dose within the patient. It is therefore prudent to include all ranges of bolus thicknesses, field sizes and treatment depths likely to be used for clinical applications during the commissioning process. For the field size correction factor, correlation was established for square field sizes and through the concept of equivalent square field size [9 - 21], field size correction factors may be determined for other non-square field sizes. The one side of a square field size used for the plots actually correspond to an equivalent square field size. Hence, if one is able to determine the equivalent square field size for a particular non-square field size, substituting the value of the determined equivalent square field size into the correlation equation gives the required field size correction factor that needs to be applied to account for the influence of field size on the thickness ratio. All the measurements were performed with isocentric (SAD) irradiation technique, because that is the treatment technique choice frequently in use at the study site. Majority of the doses measured when the treatment plans were replicated on the telecobalt machine were higher than those of the treatment plans calculated with the TPS. This shows that the proposed approach generally under-compensates the beam output. This can be attributed to challenges encountered in fabricating the compensating filter to obtained the required thickness, due to the method used in constructing the filter. Other methods for constructing the compensating filter may be used once the shape of the filter had been determined based on the proposed approach.

Though similar approach had been used with a constant thickness ratio for a particular beam energy and effects of field size, bolus/compensating filter thickness and treatment depth ignored, and had culminated in encouraging results (measured doses after transmitting through the compensator showing discrepancies within ± 5% from what were expected) for missing tissue compensation [4], using the proposed approach resulted in dose discrepancies of less than or equal to ± 3% from what were expected. Albeit the inherent uncertainties associated with film dosimetry [22, 23], incorporating the necessary corrections to account for tissue deficit/compensating filter thickness, field size and treatment depth had improved on the dose discrepancies determined. Notwithstanding this, the dose verification procedure needs to be repeated with other 2D array detectors based on ionization chamber or diode. In other related compensating filter works, some of the researcher made provisions to incorporate the effects of off-axis distance in their respective approaches in the determination of the thickness of the compensating filter, since most of their beam data were acquired on the beam central axis and compensation needed to be done at other parts of the radiation field other than on the beam central axis [24, 25]. It is also expected that if the effects of the off-axis distance are also considered in the proposed approach there will be much improvement in the output of the proposed approach. Nevertheless, there were some challenges with the proposed approach. Obtaining applied bolus thicknesses for beams with oblique incidence relative to the surface of the phantom were

quiet challenging and cumbersome. There was limitation with the thickness of bolus that could be applied, which should not be more than 14 cm, limiting the amount of tissue compensation that can be applied. The use of abutting fields where there are overlap of fields were problematic as the TPS did not allow entering of bolus for individual radiation field. Further study needs to be conducted to assess the influence of varying the constant thickness of the Perspex plate used in the determination of the field size and treatment depth correction factors.

IV. CONCLUSION

Procedures for constructing missing tissue compensator using Perspex slabs have been outlined for a telecobalt machine. The approach adopted accounts for the effects of treatment parameters (field size, treatment depth and applied bolus/compensator material thickness) in estimating the required thickness of compensator material that would produce a desired dose distribution (achieved with a bolus) within a tissue-equivalent phantom. Although similar approach had been used where the effects of the treatment parameters had been ignored with encouraging results, incorporating the effects of the treatment parameters yield more favourable results.

V. ACKNOWLEDGEMENT

This publication is an extract of a research work carried out by the principle author to enable him complete his PhD thesis, which was submitted to the Department of Physics, School of Physical Sciences, College of Agriculture and Natural Sciences, University of Cape Coast, Ghana, in partial fulfillment of a PhD degree.

VI. REFERENCES

[1]. Schlegel W, Bortfeld T, Grosu A. New technologies in radiation oncology. Springer-Verlag Berlin Heidelberg, Germany (2006).

[2]. Khan FM. Treatment Planning in Radiation Oncology, 2nd Edition, Lippincott Williams and Wilkins (2007).

[3]. Podgorsak E. B., Radiation oncology Physics: A handbook for teachers and students, International Atomic Energy Agency , IAEA (2005).

[4]. Khan FM. The Physics of Radiation Therapy. Fourth Edition. Lippincott Williams and Wilkins (2010).

[5]. Kassaee A, Bloch P, Yorke E, Altschuler MD, Rosenthal DI. Beam spoilers versus bolus for 6 MV photon treatment of head and neck cancers. Med Dosim. 25(3):127-31 (2000).

[6]. Kutcher G J, Coia L, Gillin M, Hanson W F.et al. Comprehensive QA for radiation oncology: Report of AAPM radiation therapy committee task group 40 Med. Phys. 21 (4): 581- 618 (1994).

[7]. International Electrotechnical Commission (IEC): Medical electrical equipment – Dosimeters with ionization chambers as used in radiotherapy. IEC 60731. IEC (1997).

[8]. National Institute of Standards and Technology (NIST),USA, Physical measurement laboratory: http://physics.nist.gov.

[9]. Day, M.J., A note on the calculation of dose in x-ray fields. British Journal of Radiology. 23(270): p. 368-9 (1950).

[10]. Day, M.J. and E.G. Aird, The equivalent field method for dose determinations in rectangular fields. British Journal of Radiology Suppl. 25: p. 138-51 (1996).

[11]. Bjarngard, B.E. and R.L. Siddon, A note on equivalent circles, squares, and rectangles. Med Phys. 9(2): p. 258-60 (1982).

[12]. Clarkson, J.R., A note on depth doses in fields of irregular shape. British Journal of Radiology 14: p. 265- 268 (1941).

[13]. Sathiyan, S., M. Ravikumar, and S.L. Keshava, Relative Output Factors and Absolute Equivalent Square Fields at Depths for High

Energy XRay and Gamma Ray Beams. Austral Asian Journal of Cancer. 5(4): p. 225-235 (2006).

[14]. Sterling, T., H. Perry, and J. Weinkam, Automation of radiation treatment planning. VI. A general field equation to calculate percent depth dose in the irradiated volume of a cobalt 60 beam. British Journal of Radiology, 40(474): p. 463-74 (1967).

[15]. Vadash, P. and B. Bjarngard, An equivalent-square formula for head scatter factors. Med Phys. 20(3): p. 733-4 (1993).

[16]. Monti, A.F., et al., An equivalent square method for irregular photon fields. Med Dosim. 20(4): p. 275-7 (1995).

[17]. Sanz, D.E., Accuracy limits of the equivalent field method for irregular photon fields. Phys Med Biol. 47(17): p. 3073-85 (2002).

[18]. Thomas, S.J., et al., Equivalent squares for small field dosimetry. Br J Radiol, 2008. 81(971): p. 897-901.

[19]. Araki F., et al. Dose calculation for asymmetric photon fields with independent jaws and multileaf collimators. Med Phys, 2000. 27(2): p. 340-5.

[20]. Kwa W., et al., Dosimetry for asymmetric x-ray fields. Med Phys, 1994. 21(10): p. 1599-604. Day, M.J., The equivalent field method for axial dose determinations in rectangular fields. British Journal of Radiology, 11: p. Suppl 11:95-10 (1972).

[21]. Tagoe SNA, Nani EK, Yarney J., et al. Semi-empirical equivalent field method for dose determination in midline block fields for cobalt-60 beam. Journal of Applied Science and Technology. volume 17(1-2); Pp.70-77 (2012).

[22]. Martisikova M, Ackermann B, Jakel O. Analysis of uncertainties in Gafchromic EBT film dosimetry of photon beams.; Phys. Med. Biol. 53 7013 (2008).

[23]. Devic S, Seuntjens J, Hegyi G, and Podgorsak E B et al. Dosimetric properties of improved GafChromic films for seven different digitizers. Med. Phys. 31 (9): 2392 - 2401(2004).

[24]. Haghparast A, Hashemi B, and Eivazi M T. Influence of compensator thickness, field size, and off-axis distance on the effective attenuation coefficient of a cerrobend compensator for intensity-modulated radiation therapy. Medical Dosimetry. 38; 25-29 (2013).

[25]. Iwasaki A, KuIwasaki A, Kubota M, Fujimori A, Suzaki K, Abe Y, Ono H et al. Formulation of spectra-based attenuation coefficients in water as a function of depth and off-axis distance for 4, 10 and 15MV X-ray beams. Radiation Physics and Chemistry, 72:657-661 (2005).

[26]. International Atomic Energy Agency (IAEA), IAEA-TECDOC-896. Radiation dose in radiotherapy from prescription to delivery. IAEA, Vienna, (1996).